ORGANIC PROCESS RESEARCH & DEVELOPMENT
OPR&D

pubs.acs.org/OPRD Article

Precise Preparation of a High-Purity Key Intermediate of Tazobactam

Yanan Zhou,[†] Chengjun Wu,[†] Hongzhi Ma, Jianchao Chen,* and Tiemin Sun*

Cite This: https://dx.doi.org/10.1021/acs.oprd.0c00407 Read Online

ACCESS | Metrics & More | Article Recommendations | Supporting Information

ABSTRACT: In situ IR was used to precisely prepare high-purity diphenylmethyl 6α-bromopenicillanate **8**, a key intermediate of tazobactam. **8** was obtained when 6α-bromopenicillanic acid **2** reacted with diphenyldiazomethane (DDM). **2** is unstable and must therefore react immediately with DDM upon preparation. DDM is also unstable. As DDM decomposes rapidly upon preparation, the DDM content cannot be precisely determined using high-performance liquid chromatography (HPLC) or gas chromatography (GC). Therefore, good yield and purity are difficult to obtain, resulting in large batch-to-batch variations (yield 69.3−82.8%, purity 89.8−98.4%) for **8**. The developed preparation method for **8** involved the use of in situ IR to monitor the reaction process and achieved good results (82.7−83.1% yield and 97.3−98.5% purity). This method was also used to prepare the key intermediate for the synthesis of cephalosporin derivatives, which have high industrial value.

KEYWORDS: *diphenylmethyl 6α-bromopenicillanate, diphenyldiazomethane, purity drift, in situ IR, cephalosporin derivatives*

1. INTRODUCTION

Tazobactam (**1**) is an orally effective penicillin antibiotic with a broad spectrum of antibacterial activity against both Gram-positive and Gram-negative organisms[1−4] and is typically added to certain antibiotics to lower the antimicrobial resistance of bacteria.[5] For example, a combination of tazobactam and piperacillin can be used to treat infections caused by *Pseudomonas aeruginosa*.[6−8]

Scheme 1 illustrates the most widely used synthetic route for tazobactam.[9,10]

One of the key intermediates in the preparation of tazobactam is 6α-bromopentamidine sulfoxide dibenzoate **3**. **3** was originally synthesized using a three-step process with 6-aminopenicilanic acid (6-APA) as a starting material.[9] The 6α-bromopenicillanic acid **2** was isolated from the products of a Sandmeyer reaction. **2** was oxidized by peracetic acid to sulfoxide **7**. Peracetic acid and benzophenone hydrazine (BPH) were added to the reaction mixture, and the resulting esterification produced **3** without isolation. Although this procedure is generally used in industry, several problems need to be solved urgently. First, an overoxidation product (**3′**) is produced, irrespective of any countermeasures implemented. Second, a very poor esterification yield is obtained using a low concentration of peroxyacetic acid (20%). Therefore, a higher concentration of peracetic acid (40%) is needed, the preparation of which poses extreme safety hazards for industrial production.[11]

Peracetic acid/BPH use has been circumvented by using diphenylmethanol and diphenyldiazomethane (DDM) as effective alkylation reagents for carboxylic acids during esterification;[12,13] however, these alternative reagents have not yet been used in industrial production (Scheme 2). The difficulty of removing the byproduct 1,3-dicyclohexylurea (**9**) from the reaction system diminishes the efficiency of using Route A for large-scale processes.[14] Route B consists of replacing BPH by DDM during esterification. This method does not have some of the drawbacks of existing routes, such as peracetic acid (40%) use, and has a considerably shorter reaction time. However, the instability of DDM prevents the DDM content from being precisely ascertained using general high-performance liquid chromatography (HPLC) or gas chromatography (GC).[15−18] In addition, DDM must be synthesized immediately before use and cannot be stored. Ketone has been found to be the main byproduct during DDM preparation. Therefore, the content of different DDM batches has been found to be variable. This result is shown in Table 2. That is, the 1.4 equiv of DDM is not always optimal. Optimization of the reaction conditions for each DDM batch reduces large-scale esterification efficiency. Route B also involves the synthesis of compound **2** by diazotization−bromination of 6-APA. The absence of aromatic conjugation results in an unstable diazonium salt, increasing the yield of byproducts in the reaction system. In addition, the instability of **2** necessitates reaction with DDM without purification to yield **8**. The reaction mechanism shows that one molecule of **2** reacts with one molecule of DDM to produce one molecule of **8**. When a 1:1 ratio of the two reactants cannot be guaranteed (that is, there is an excess of either reactant), side reactions occur that affect product purity, resulting in a purity range of 89.5−98.4% for **8**.[19] Thus, an accurate determination of the concentration of these two reactants is key to increasing

Received: September 14, 2020

https://dx.doi.org/10.1021/acs.oprd.0c00407
Org. Process Res. Dev. XXXX, XXX, XXX−XXX

Scheme 1. Synthetic Route for Tazobactam

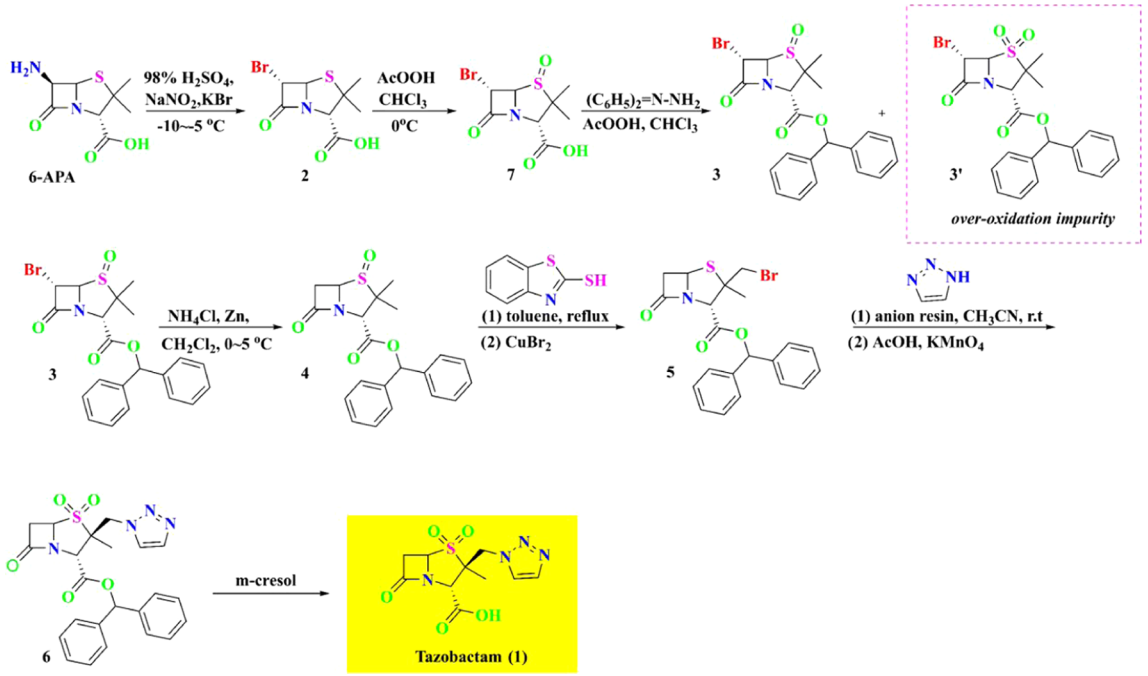

Scheme 2. Alternative Routes to Produce Bromopentamidine Sulfoxide Dibenzoate (3)

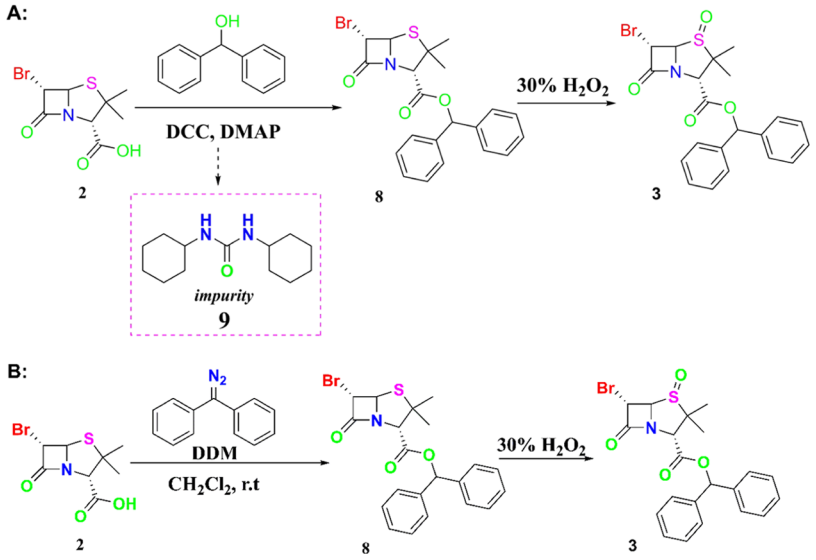

product purity. The aforementioned problems have challenged chemists for decades and motivated us to explore a new strategy for the transformation of reactants.[20−23]

Recent developments in process analytical technology (PAT),[24,25] especially in situ infrared spectroscopy (IR),[26,27] have made it possible to follow a reaction in real time, whereby quality by design (QbD)[28] principles are used to obtain an in-depth understanding of chemical processes.[29,30] To the best of our knowledge, in situ IR has been used to observe a multicomponent synthesis process for which the reactant content cannot be accurately determined, whereas previous studies have been fundamental in nature and have not been applied to industrial production. We developed a preparation method for **8** using in situ IR to monitor the reaction process, with good results (82.7−83.1% yield and 97.3−98.5% purity) at the kilogram scale. Online monitoring was used for the real-time tracking of changes in the contents of the reactants and products. Precise quantities of DDM and compound **2** could be added to the reaction system. The reaction endpoint could be accurately controlled. Large fluctuations in the yield and purity during esterification were effectively eliminated. The method was also used to prepare a key intermediate for the synthesis of cephalosporin derivatives, which have high industrial value.

2. RESULTS AND DISCUSSION

2.1. Optimization and Evaluation of the Esterification Process. First, the existing synthetic method for compound **8** (Scheme 2B) was evaluated. Compound **2** was rapidly consumed during the dropwise addition of DDM. The yield of **8** was initially improved from 52.4 to 78.9% by increasing

https://dx.doi.org/10.1021/acs.oprd.0c00407
Org. Process Res. Dev. XXXX, XXX, XXX−XXX

the DDM equivalent from 0.9 to 1.4 (Table 1, entries 1−5). Further increase in the DDM equivalent to 1.5 did not improve the yield, and the purity decreased, indicating that the optimal DDM equivalent was 1.4. As the related byproduct benzhydryl ethyl ether can form in a protic solvent,[31] several aprotic solvents (CH_3CN, EtOAc, tetrahydrofuran (THF), and toluene) were screened, none of which produced a clear change in the yield (Table 1, entries 7−10). The results of a temperature survey are presented in Table 1 (entries 11−13). Low temperatures decreased the overall rate, whereas high temperatures increased the DDM decomposition rate, both of which decreased the yield. Finally, four identical experiments were performed on different DDM batches under the optimal conditions (Table 1, entries 14−17). The resulting significant variations in the purity of compound **8** (89.8−98.4%, RSD = 4.07%) are not conducive to scale up production.

Table 1. Optimization of the Esterification Process[a]

entry	$n_{(DDM)}/n_{(6\text{-APA})}$	solvent	temp. (°C)	yield (%)	purity (%)
1[b]	0.9	CH_2Cl_2	20	52.4	85.4
2[b]	1.0	CH_2Cl_2	20	58.2	89.5
3[b]	1.2	CH_2Cl_2	20	68.5	94.0
4[b]	1.3	CH_2Cl_2	20	75.2	95.2
5[b]	**1.4**	**CH_2Cl_2**	**20**	**78.9**	**98.2**
6[b]	1.5	CH_2Cl_2	20	78.4	90.6
7[b]	1.4	CH_3CN	20	78.6	97.7
8[b]	1.4	EtOAc	20	78.2	97.2
9[b]	1.4	THF	20	77.7	98.3
10[b]	1.4	toluene	20	77.9	97.3
11[b]	1.4	CH_2Cl_2	0	71.4	96.4
12[b]	1.4	CH_2Cl_2	−10	69.7	92.2
13[b]	1.4	CH_2Cl_2	35	71.7	89.5
14[c]	1.4	CH_2Cl_2	20	69.3	98.4
15[c]	1.4	CH_2Cl_2	20	79.0	97.1
16[c]	1.4	CH_2Cl_2	20	82.8	89.8
17[c]	1.4	CH_2Cl_2	20	76.1	93.6

[a]Bold values indicate that the 1.4 equiv of DDM is not always optimal reaction conditions. [b]The same batch of DDM was needed for the optimization conditions to reduce the variables in the experiment. [c]The different batches of DDM.

DDM instability was quantitatively assessed using both stable 2-(3,4-dimethoxyphenyl)acetic acid **10** and benzophenone hydrazine to yield the corresponding acetic acid ester **11**. Although the experimental conditions were strictly controlled, variations in the purity of compound **11** were still observed (Table 2). This result confirmed the variable contents of different DDM batches.

Oxidants can be used to prepare DDM from benzophenone hydrazine. Various oxidants are available for this purpose.[21,32−34] Manganese dioxide was chosen in this study because of its recyclability.

2.2. Process Improvements. In situ IR was used to monitor the esterification process, enabling the precise determination of the reaction endpoint and control of the quantities of DDM and **2**. Although in situ IR has been used to monitor diazonane-related reactions, previous studies have been fundamental in nature and have not been applied to industrial production.[35−37] In situ IR was used in this study to obtain the spectra of the reactants and products to accurately track the reaction evolution. Dichloromethane (CH_2Cl_2) was placed in an oven-dried three-necked flask, which was fitted with a DiComp probe; the infrared spectrum of CH_2Cl_2 was then collected. Compound **2** was then added to the flask, and the IR spectra of **2** were obtained by subtracting the solvent background (CH_2Cl_2). The operations described above were repeated to collect the IR spectra of DDM and compound **8**. The infrared absorption characteristic peaks of the collected samples were processed within the 1750−900 cm^{-1} high infrared absorption range using iC IR 4.0 operating software (Figure 1).

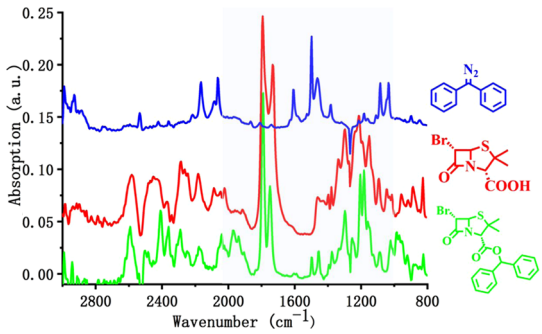

Figure 1. IR spectra of 6α-bromopenicillic acid **2** (red), diphenylmethyl 6α-bromopenicillanate **8** (green), and **DDM** (blue): the blue background represents areas for which characteristic peaks of collected samples were within the 1750−900 cm^{-1} high infrared absorption range.

The peak at 1792 cm^{-1} was assigned to the stretching vibration of the C═O bond in the β-lactam ring for both compounds **2** and **8**. The absorption peaks at $\nu_{C=O}$ 1732 cm^{-1} and $\nu_{C=O}$ 1748 cm^{-1} were assigned to the carboxylic acid in compound **2** and the ester in compound **8**, respectively. The 2035 cm^{-1} peak originating from C═N stretching (the most intense absorption for DDM) was masked by absorptions

Table 2. Yield and Purity of Product 11 in Different Batches

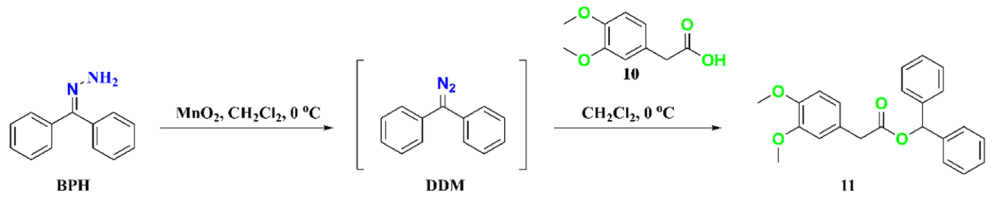

entry	$n_{(BPH)}/n_{(compound\ 10)}$	output (g)	total yield (%)	HPLC purity (% area)
1	1.0	2.58	69.91	96.79
2	1.0	3.0	81.3	99.12
3	1.0	2.80	75.88	97.47

https://dx.doi.org/10.1021/acs.oprd.0c00407
Org. Process Res. Dev. XXXX, XXX, XXX−XXX

arising from diamond transmits IR (2200−1900 cm^{-1}) of the attenuated total refraction (ATR) probe, but the peaks of the benzene ring in DDM could be tracked. The stretching vibration peaks of the benzene ring in DDM appeared at 1596, 1499, and 1461 cm^{-1}.

The complex composition of the reaction system resulted in significant overlap among the absorption peaks, making it difficult to accurately observe the characteristic peaks of the three components in the original online infrared spectrum. Second derivative infrared spectroscopy was applied to distinguish among the characteristic peaks of the components in the esterification reaction more clearly. The second derivative spectrum is shown in Figure 2A,B. The objective of this series of experiments was to use in situ IR to accurately track the trends in the evolution of each component over time (Figure 3).

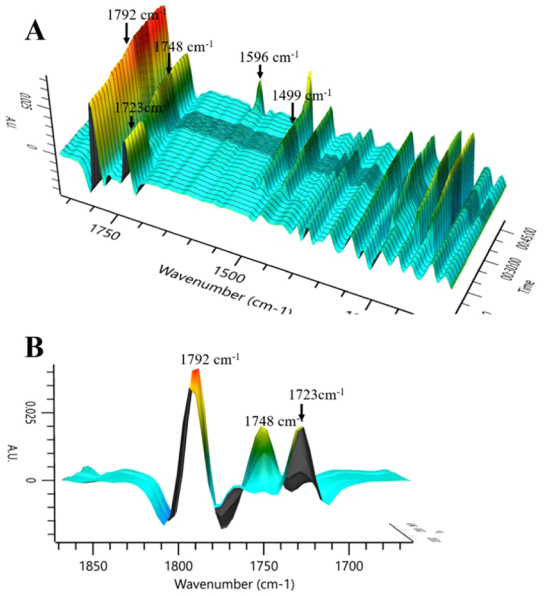

Figure 2. Online infrared three-dimensional spectrum acquired during an esterification reaction as a function of time and wavelength after second derivative treatment: (A) IR stack plot of the entire reaction process and (B) IR stack plot of changes in the main characteristic peaks.

2.3. Inline Monitoring of the Esterification Process by In Situ IR. Figure 3A shows a plot of the peak heights at 1723 cm^{-1} (red curve) and 1748 cm^{-1} (green curve) (corresponding to the C═O stretch of the carboxylic acid in compound **2** and the ester carbonyl group in **8**, respectively) versus the reaction time. Point **a** corresponds to the addition of compound **2** dissolved in CH_2Cl_2 to the reaction mixture. After the system stabilized, DDM was added at point **b**. The red curve decreased and the green curve increased upon DDM addition, indicating that the reaction occurred immediately with the consumption of compound **2** and the formation of product **8**. Figure 3C shows that DDM addition was accompanied by a sharp increase in the temperature over the **b**−**c** section. Considering the instability of compound **2** at high temperatures, the addition rate of DDM was slowed down at **c**, and the temperature increase ceased. If the drop speed is not adjusted in time, an explosion accident can easily occur during industrial production.

DDM was added dropwise continuously at **d**, and the C═O stretching vibration peaks at 1748 and 1723 cm^{-1} plateaued at point **e**. DDM addition was terminated at point **e**. To ascertain whether point **e** was the reaction endpoint, DDM was then added dropwise at point **f**. Figure 3A shows an increase in the intensity of the C═C stretching vibration absorption peak from the DDM benzene ring at 1596 cm^{-1} (blue curve) but no change in the absorption peaks related to compounds **8** and **2**. Therefore, point **e** was concluded to be the reaction endpoint, as determined by in situ IR. Notably, the esterification process between compound **2** and DDM was completed in 20 min, with 60% of compound **2** being consumed in approximately 7 min, as shown by the superposition of the three IR spectra at 1, 7, and 17 min in Figure 3B,D,[36] which was considerably less than the 20 h reported in the literature[13] and indicates a considerably reduced energy consumption and the prevention of impurity formation to the greatest possible extent.

To further confirm that point **e** was the reaction endpoint, samples were collected at the **d**−**e**, **e**−**f**, and **f**−**g** segments, and HPLC was used to determine the purity of product **8**. When the reaction was at the **d**−**e** segment, compound **2** remained, and the purity of product **8** was 90.2% (Figure S1); the maximum purity of **8** of 98.9% was obtained at the **e**−**f** section (Figure S2). More impurities were found from HPLC of the sample at the **f**−**g** segment, and the purity of **8** declined to 87.5%, mainly because of the presence of excess DDM (Figure S3).

2.4. Thermogravimetric Analysis (TGA) of DDM. A TGA experiment was performed to determine the feasibility of using DDM in a scaled process (Figure 4). The DDM thermograms contained two separate degradation steps, or stages, with two maximum rate peaks that can be clearly seen in the corresponding DTG curves. DDM weight losses of 10.6795 and 83.3573% occur over the temperature ranges of 85−145 and 235−350 °C, respectively. The first step corresponds to the dissociation of the diazo into N_2 gas and a highly reactive carbene, along with other byproducts, whereas the second step corresponds to the degradation of residues. Therefore, DDM is thermally stable under the experimental conditions.

2.5. Process Scale-Up. The efficiency of the developed preparation method (Scheme 3) was verified using other batches, and the results are presented in Table 3. The purity of compound **8** was in the 97.3−98.5% range, with a relative standard deviation (RSD) of 0.47%, showing the effective elimination of large fluctuations in the product purity.

2.6. Application to Cephalosporin Derivatives. The problems encountered in cefdinir preparation also exist in the preparation of cephalosporin derivatives.[38] The typical use of excess DDM to yield diphenylmethyl 7β-phenylacetamido-3-hydroxymethyl-3-cephem-4-carboxylate **13** both reduces the purity of **13** and increases production costs. We extended this method to prepare **13**, an important intermediate for the synthesis of cephalosporin derivatives, with satisfactory results, as shown in Table 4 (RSD = 0.36%).

3. CONCLUSIONS

Diphenylmethyl 6α-bromopenicillanate **8**, a key intermediate of tazobactam, was prepared using in situ IR to monitor the reaction process, with good results (82.7−83.1% yield and 97.3−98.5% purity) at the kilogram scale. The effective synthetic method was established for various contents of several raw materials. The use of in situ IR is key for the

https://dx.doi.org/10.1021/acs.oprd.0c00407
Org. Process Res. Dev. XXXX, XXX, XXX−XXX

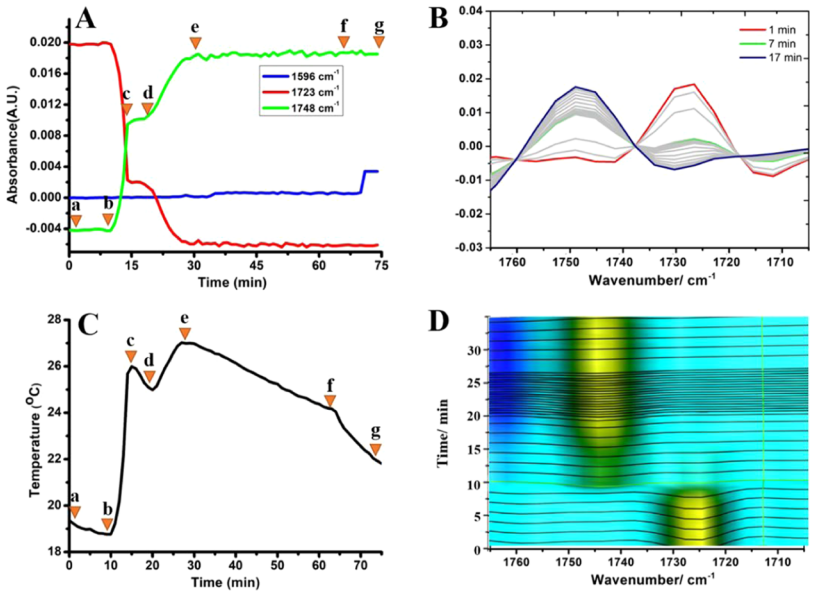

Figure 3. (A) Changes in absorbance at 1723 cm^{-1} (red curve), 1748 cm^{-1} (green curve), and 1596 cm^{-1} (blue curve) plotted against reaction time during formation of product **8**; (B, D) time-domain ATR-IR spectra during esterification, where superimposed IR spectra at 1, 7, and 17 min show conversion of compound 2 to product 8 (from 1723 to 1748 cm^{-1}) upon DDM addition; and (C) reaction temperature as a function of time.

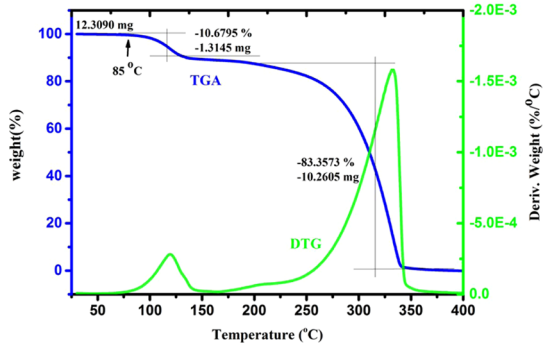

Figure 4. TGA (blue) and DGT (green) thermograms for DDM: blue line, observed; and green line, calculated.

success of this process because the accurate control of the DDM quantity and the precise determination of the reaction endpoint circumvent the inconclusive determination of the contents of DDM and compound **2**. Moreover, we found that the esterification could be completed within 20 min using in situ IR, which considerably reduced energy consumption and prevented the growth of impurities. The developed method was used to prepare the key intermediate in the synthesis of cefdinir. The developed protocol can instantaneously detect profiles of species that are otherwise undiscernible or cannot be easily measured offline.

Table 3. Purity of Product 8 in Different Batches

entry[a]	batch size of 6-APA (kg)	output (kg)	total yield (%)	HPLC purity (% area)
1	2.16	3.69	82.9	98.2
2	2.16	3.70	83.1	97.7
3	10.8	18.47	82.9	97.3
4	10.8	18.43	82.7	98.5

[a]The different batches of DDM.

Scheme 3. Overall Process Scheme

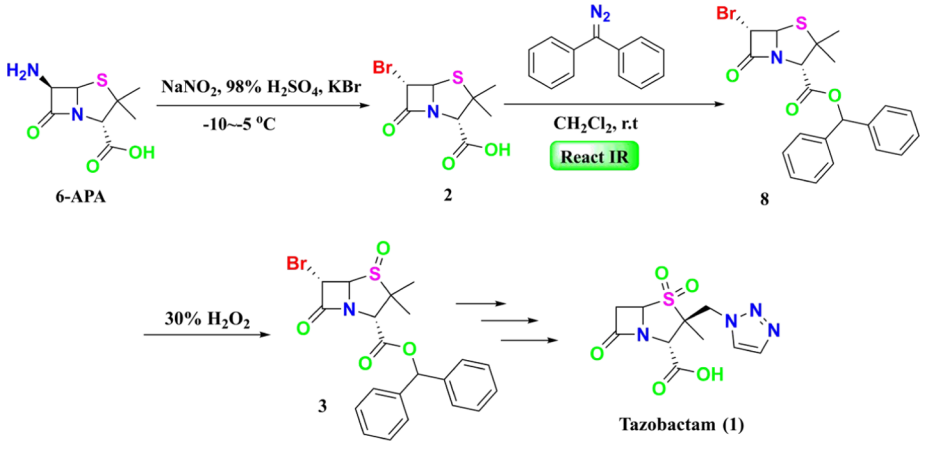

https://dx.doi.org/10.1021/acs.oprd.0c00407
Org. Process Res. Dev. XXXX, XXX, XXX−XXX

Table 4. Purity of Product 13 in Different Batches

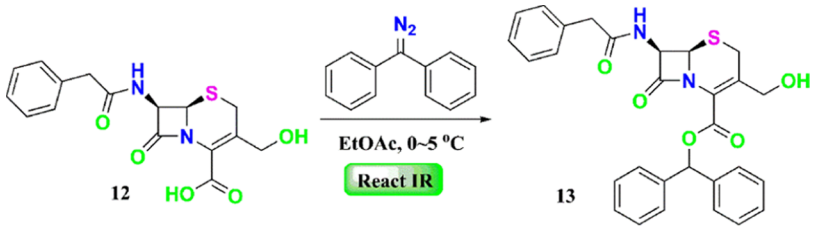

entry[a]	batch size of **12** (g)	output (g)	total yield (%)	HPLC purity (% area)
1	5.0	6.27	85.0	98.83
2	5.0	6.18	83.7	99.06
3	20.0	24.83	84.9	98.27
4	20.0	24.34	83.2	98.98

[a]The different batches of DDM.

4. EXPERIMENTAL SECTION

4.1. General. All chemicals were commercially available and were used directly without further purification. The EliteP230p series instrument (column: Hyper ODS2 C18 (250 mm × 20 mm); pump: P230p; detector: UV230II, Dalian Elite Analytical Instruments Co., Ltd., China) was used to monitor the reaction. Proton nuclear magnetic resonance (^{1}H NMR) spectra and carbon-13 nuclear magnetic resonance (^{13}C NMR) spectra were recorded using a Bruker 400 MHz spectrometer. Infrared spectra were obtained on an FTIR spectrometer (EQUINOX55, Bruker, Germany) at 1.0 cm^{-1} resolution and are reported in wavenumbers. All in situ infrared spectra were collected using an IN-SITU IR (ReactIR 15, Mettler Toledo, Redmond, VA) equipped with an ATR diamond sensor probe interfaced with the Mettler iC IR 4.0 synthesis workstation. A TGA (TGA 2 (SF), Mettler Toledo, Switzerland) thermogravimetric analyzer was employed for thermogravimetric analysis at a heating rate of 5 K min^{-1} under nitrogen from 303.2 to 673.2 K.

4.2. Preparation of Diphenylmethyl 2-(3,4-dimethoxyphenyl)acetate (11). A solution of benzophenone hydrazone (2.0 g, 0.01 mol) in dichloromethane (30 mL) was cooled to 0 °C. Activated manganese dioxide (2.66 g, 0.03 mol) was added to the solution in three portions. The reaction mixture was warmed to room temperature and maintained under stirring for 1.5 h. The mixture was filtered, and the red filtrate was used in the next step without purification.

2-(3,4-dimethoxyphenyl)acetic acid (2 g, 0.01 mol) was added under stirring to a solution of the filtrate at room temperature, which was then maintained under stirring for 1 h. The solvent was evaporated, and the residue was crystallized from ether/*n*-hexane(1:1 v/v) to yield **11** as a white solid (2.8 g, 75.88%). ^{1}H NMR (400 MHz, dimethyl sulfoxide (DMSO)-d_6) δ 7.60−7.12 (m, 10H), 6.9 (1H, d, J = 5.5 Hz, ArH), 6.89 (1H, s, $CHPh_2$), 6.80 (2H, ArH), 3.73 (s, 5H), 3.69 (s, 3H).

4.3. Scale-Up: 6α-Bromopenicillanic Acid (2). A solution of KBr (30 kg, 252.1 mol) in water (117.5 kg) was placed in a 500-L reactor, and 98% H_2SO_4 (8.75 kg, 87.43 mol), EtOH (95%, 21.4 kg), and 6-APA (10.8 kg, 50 mol) below −5 °C with cold brine were added to the reaction vessel. Next, a solution of $NaNO_2$ (5 kg) in H_2O (20 kg) was slowly added over 1 h at −15 to −10 °C, and the reaction mixture was maintained at this temperature for 4 h, at which point HPLC analysis indicated <0.5% of 6-APA. The reaction mixture was diluted with dichloromethane (50 kg). The aqueous phase was washed with CH_2Cl_2 (12.5 kg × 2). The combined organic phase was washed with a saturated aqueous sodium chloride solution (1 × 12.5 kg) and then dried over anhydrous Na_2SO_4 (14.0 kg). The solution was filtered, the filtrate was placed in a 250-L stirred reactor, and used without purification in the next step.

4.4. Preparation of Diphenyldiazomethane (DDM). A solution of benzophenone hydrazone (15 kg, 76.43 mol) in dichloromethane (70 kg) was cooled to 0 °C. Activated manganese dioxide (19.93 kg, 229.29 mol) was added in three portions. The reaction mixture was warmed to room temperature and stirred continuously for 1.5 h. After the centrifuge separated, the red filtrate was concentrated to one-fifth of its original volume and used in the next step without purification.

4.5. Preparation of Diphenylmethyl 6α-Bromopenicillanate (8). In the 250 L reaction tank equipped with an in situ IR ATR probe, the newly prepared DDM was added dropwise to the filtrate through an overhead tank. Addition of DDM was stopped when the in situ IR indicated reaction completion. After the solution was concentrated to one-fifth of its original volume, it was charged with CH_3OH (125 L) over 2 h at 0 °C, resulting in a white slurry. The slurry was filtered and the filter cake was washed with cold methanol (12.5 L), and then dried under vacuum (45 °C, −0.095 mPa) for 4 h to give **8** as a white solid (18.43 kg, 82.7%). ^{1}H NMR (400 MHz, $CDCl_3$) δ 7.39−7.27 (m, 10H), 6.94 (s, 1H), 5.43 (d, J = 1.3 Hz, 1H), 4.80 (d, J = 1.4 Hz, 1H), 4.63 (s, 1H), 1.59 (s, 3H), 1.26 (s, 3H). ^{13}C NMR (400 MHz, $CDCl_3$) δ 167.32, 166.06, 139.04, 128.68, 128.65, 128.46, 128.31, 127.51, 127.10, 78.62, 70.73, 70.02, 65.27, 49.56, 34.24, 25.50. IR (neat): 3030, 2977, 2919, 1778, 1744, 1495, 1454, 1293, 1203, 1180, 968, 745, 705, 593, 546 cm^{-1}. ESI-MS: m/z 446.36.

4.6. Preparation of Diphenylmethyl 7β-phenylacetamido-3-hydroxymethyl-3-cephem-4-carboxylate (13). The esterification of the acid (**12**) (5 g) with diphenyldiazomethane was carried out as above to give **13** as a white solid (6.27 g, 85.0%). ^{1}H NMR (400 MHz, DMSO-d_6) δ 9.12 (d, J = 8.4 Hz, 1H), 7.66−7.16 (m, 15H), 6.90 (s, 1H), 5.72 (dd, J = 8.3, 4.7 Hz, 1H), 5.15 (t, 1H), 5.11 (d, J = 4.8 Hz, 1H), 4.21 (d, 2H), 3.61 (s, 2H), 3.52 and 3.56 (m, 2H). ^{13}C NMR (400 MHz, DMSO-d_6) δ 171.43, 165.70, 161.34, 140.52, 140.45, 136.29, 134.87, 129.48, 128.98, 128.85, 128.69, 128.31, 128.24, 127.23, 127.03, 126.96, 122.45, 78.80, 60.24, 59.37, 58.18, 42.06, 26.04. ESI-MS: m/z 537.21 [M + Na]$^+$.

https://dx.doi.org/10.1021/acs.oprd.0c00407
Org. Process Res. Dev. XXXX, XXX, XXX−XXX

■ ASSOCIATED CONTENT

Supporting Information

The Supporting Information is available free of charge at https://pubs.acs.org/doi/10.1021/acs.oprd.0c00407.

HPLC spectra of diphenylmethyl 6α-bromopenicillanate **8** (**d**−**e** as the reaction endpoint during the synthesis process; **e**−**f** as the reaction endpoint during the synthesis process; **f**−**g** as the reaction endpoint during the synthesis process; large-scale experiment); HPLC spectrum of diphenylmethyl 2-(3,4-dimethoxyphenyl)-acetate **11** and diphenylmethyl 7β-phenylacetamido-3-hydroxymethyl-3-cephem-4-carboxylate **13**; infrared spectrum, and ^{1}H NMR and ^{13}C NMR spectra of diphenylmethyl 6α-bromopenicillanate **8**; ^{1}H NMR spectra of diphenylmethyl 2-(3,4-dimethoxyphenyl)-acetate **11**; and ^{1}H NMR and ^{13}C NMR spectra of diphenylmethyl 7β-phenylacetamido-3-hydroxymethyl-3-cephem-4-carboxylate **13** (PDF)

■ AUTHOR INFORMATION

Corresponding Authors

Tiemin Sun − *Key Laboratory of Structure-Based Drug Design and Discovery, Shenyang Pharmaceutical University, Ministry of Education, Shenyang 110016, P. R. China*; orcid.org/0000-0002-9981-0243; Email: suntiemin@126.com

Jianchao Chen − *Key Laboratory of Structure-Based Drug Design and Discovery, Shenyang Pharmaceutical University, Ministry of Education, Shenyang 110016, P. R. China*; Email: chenjianchaosyphu@163.com

Authors

Yanan Zhou − *Key Laboratory of Structure-Based Drug Design and Discovery, Shenyang Pharmaceutical University, Ministry of Education, Shenyang 110016, P. R. China*

Chengjun Wu − *Key Laboratory of Structure-Based Drug Design and Discovery, Shenyang Pharmaceutical University, Ministry of Education, Shenyang 110016, P. R. China*

Hongzhi Ma − *Key Laboratory of Structure-Based Drug Design and Discovery, Shenyang Pharmaceutical University, Ministry of Education, Shenyang 110016, P. R. China*

Complete contact information is available at: https://pubs.acs.org/10.1021/acs.oprd.0c00407

Author Contributions

†Y.Z. and C.W. contributed equally to this work.

Notes

The authors declare no competing financial interest.

■ REFERENCES

(1) Setti, E. L.; Fiakpui, C.; Phillips, O. A.; Czajkowski, D. P.; Atchison, K.; Micetich, R. G.; Maiti, S. N.; et al. Chemical modification of tazobactam—synthesis of 2β-[(4-substituted)-1,2,3-triazol-1-yl]methyl penicillnic acid sulfone derivatives. *J. Antibiot.* **1995**, *48*, 1320−1329.

(2) Zaghloul, I.; Kuck, N.; Yacobi, A. The effect of tazobactam on the pharmacokinetics and the antibacterial activity of piperacillin in dogs. *Int. J. Pharm.* **1997**, *153*, 115−121.

(3) Padayatti, P. S.; Anjaneyulu, S.; Monica, A. T.; Marion, S. H.; Marianne, P. C.; Vernon, E. A.; Paul, R. C.; Christopher, R. B.; Robert, A. B.; John, D. B.; Focco, A. Rational design of a β-lactamase inhibitor achieved via stabilization of the trans-Enamine intermediate: 1.28 Å crystal structure of *wt* SHV-1 complex with a Penam Sulfone. *J. Am. Chem. Soc.* **2006**, *128*, 13235−13242.

(4) Yang, Y.; Janota, K.; Tabei, K.; Huang, N.; Siegel, M. M.; Lin, Y. I.; Rasmussen, B. A.; Shlaes, D. M. Mechanism of inhibition of the class A β-lactamases PC1 and TEM-1 by Tazobactam: Observation of reaction products by electrospray ionization mass spectrometry. *J. Biol. Chem.* **2000**, *275*, 26674−26682.

(5) Livermore, D. M. β-Lactamases in Laboratory and Clinical Resistance. *Clin. Microbiol. Rev.* **1995**, *8*, 557−584.

(6) Bryson, H. M.; Brogden, R. N. Piperacillin/tazobactam. a review of its antibacterial activity, pharmacokinetic properties and therapeutic potential. *Drugs* **1994**, *47*, 506−535.

(7) Buynak, J. D. Understanding the longevity of the β-lactam antibiotics and of antibiotic/β-lactamase inhibitor combinations. *Biochem. Pharmacol.* **2006**, *71*, 930−940.

(8) Yang, Y.; Rasmussen, B. A.; Shlaes, D. M. Class A β-lactamases—enzyme-inhibitor interactions and resistance. *Pharmacol. Ther.* **1999**, *83*, 141−151.

(9) Micetich, R. G.; Maiti, S. N.; Spevak, P.; Tanaka, M.; Yamazaki, T.; Ogawa, K. Synthesis of 2β-azidomethylpenicillin-1,1-diocides and 3β-azido-3α-methylcepham-1,1-dioxides. *Synthesis* **1986**, *4*, 292−296.

(10) Deshpande, P. B.; Udayampalayam, P. S.; Karale, S. N.; Kannappan, J.; Gnanaprakasam, A. A Process for the Preparation of Benzyl-2-oxo-4-(heteroaryl)dithio-alpha-isoprenyl-1-azetidineazetate Derivatives. WIPO Patent WO2004039776A22004.

(11) Kitis, M. Disinfection of wastewater with peracetic acid: a review. *Environ. Int.* **2004**, *30*, 47−55.

(12) Xu, W. L.; Li, Y. Z.; Zhang, Q. S.; Zhu, H. S. A new approach to the synthesis of tazobactam using an organosilver compound. *Synthesis* **2005**, *3*, 442−446.

(13) Buynak, J. D.; Chen, H. S. Inhibitors of Serine and Metallo-β-Lactamases. WIPO Patent WO20030871052003.

(14) Tian, Z. Y.; Du, G. J.; Xie, S. Q.; Zhao, J.; Gao, W. Y.; Wang, C. J. Synthesis and bioevaluation of 5-fluorouracil derivatives. *Molecules* **2007**, *12*, 2450−2457.

(15) Maurya, R. A.; Park, C. P.; Lee, J. H.; Kim, D. P. Continuous In Situ Generation, Separation, and Reaction of Diazomethane in a Dual-Channel Microreactor. *Angew. Chem., Int. Ed.* **2011**, *50*, 5952−5955.

(16) Muhammad, I. J.; Matthias, B. Diphenyldiazomethane. *Org. Synth.* **2008**, *85*, 189−195.

(17) Rendina, V. L.; Kingsbury, J. S. Titration of nonstabilized diazoalkane solutions by fluorine NMR. *J. Org. Chem.* **2012**, *77*, 1181−1185.

(18) McGrath, N. A.; Andersen, K. A.; Davis, A. K. F.; Lomax, J. E.; Raines, R. T. Diazo compounds for the bioreversible esterification of proteins. *Chem. Sci.* **2015**, *6*, 752−755.

(19) Deshpande, A. D.; Baheti, K. G.; Chatterjee, N. R. Degradation of β-lactam Antibiotics. *Curr. Sci.* **2004**, *87*, 1684−1695.

(20) Bauer, J.; Hou, L. L.; Kistemaker, J. C. M.; Feringa, B. L. Tuning the Rotation Rate of Light-Driven Molecular Motors. *J. Org. Chem.* **2014**, *79*, 4446−4455.

(21) Javed, M. I.; Brewer, M. Diazo Preparation via Dehydrogenation of Hydrazones with "Activated" DMSO. *Org. Lett.* **2007**, *9*, 1789−1792.

(22) Hiskey, R. G.; Adams, J. B. Sulfur-Containing Polypeptides. I. Use of the N-Benzhydryloxycarbonyl Group and the Benzhydryl Ester. *J. Am. Chem. Soc.* **1965**, *87*, 3969−3973.

(23) Oshima, T.; Nishioka, R.; Nagai, T. Facile synthetic methods of acetals and crown ethers from the reaction of diphenyldiazomethane with 2,3-dichloro-5,6-dicyanobenzoquinone in the presence of alcohols. *Tetrahedron Lett.* **1980**, *21*, 3919−3922.

(24) Caron, S.; Thomson, N. M. Pharmaceutical Process Chemistry; Evolution of a Contemporary Data- Rich Laboratory Environment. *J. Org. Chem.* **2015**, *80*, 2943−2958.

(25) Chanda, A.; Daly, A. M.; Foley, D. A.; LaPack, M. A.; Mukherjee, S.; Orr, J. D.; Reid, G. L.; Thompson, D. R.; Ward, H. W. Industry Perspectives on Process Analytical Technology: Tools and Applications in API Development. *Org. Process Res. Dev.* **2015**, *19*, 63−83.

(26) Eisenbeis, S. A.; Chen, R.; Kang, M.; Barrila, M.; Buzon, R. Utilization of ReactIR in Fit for Purpose Process Enablement. *Org. Process Res. Dev.* **2015**, *19*, 244−248.
(27) Dreimann, J. M.; Kohls, E.; Warmeling, H. F. W.; Stein, M.; Guo, L. F.; Garland, M.; Dinh, T. N.; Vorholt, A. J. In Situ Infrared Spectroscopy as a Tool for Monitoring Molecular Catalyst for Hydroformylation in Continuous Processes. *ACS Catal.* **2019**, *9*, 4308−4319.
(28) am Ende, D.; Bronk, K. S.; Mustakis, J.; O'Connor, G.; Santa Maria, C. L.; Nosal, R.; Watson, T. J. N. API Quality by Design Example from the Torcetrapib Manufacturing Process. *J. Pharm. Innovation* **2007**, *2*, 71−87.
(29) Fukui, Y.; Oda, S.; Suzuki, H.; Hakogi, T.; Yamada, D.; Takagi, Y.; Aoyama, Y.; Kitamura, H.; Ogawa, M.; Kikuchi, J. Process Optimization of Aldol-Type Reaction by Process Understanding Using in Situ IR. *Org. Process Res. Dev.* **2012**, *16*, 1783−1786.
(30) Marziano, I.; Sharp, D. C. A.; Dunn, P. J.; Hailey, P. A. On-Line Mid-IR Spectroscopy as a Real-Time Approach in Monitoring Hydrogenation Reactions. *Org. Process Res. Dev.* **2000**, *4*, 357−361.
(31) Roberts, J. D.; Watanabe, W. The Kinetics and Mechanism of the Acid-Catalyzed Reaction of Diphenyldiazomethane with Ethyl Alcohol. *J. Am. Chem. Soc.* **1950**, *72*, 4869−4879.
(32) Curini, M.; Rosati, O.; Pisani, E.; et al. Preparation of Diphenylmethyl Esters by Oxone Oxidation of Benzophenone Hydrazone. *Tetrahedron Lett.* **1997**, *38*, 1239−1240.
(33) Eastlick, D. T. Oxidation of Hydrazones to the Corresponding Diazo Compounds in the Presence of a Phase Transfer and an Oxidation Catalyst which is Iodine, an Iodine or an Iodonium Salt. U.S. Patent US725,2341976.
(34) Perusquía-Hernández, C.; Lara-Issasi, G. R.; Frontana-Uribe, B. A.; Cuevas-Yaez, E. Synthesis and esterification reactions of aryl diazomethanes derived from hydrazone oxidations catalyzed by Tempo. *Tetrahedron Lett.* **2013**, *54*, 3302−3305.
(35) Gross, E.; Shu, X. Z.; Alayoglu, S.; Bechtel, H. A.; Martin, M. C.; Toste, F. D.; Somorjai, G. A. In situ IR and X-ray high spatial-resolution microspectroscopy measurements of multistep organic transformation in flow microreactor catalyzed by Au nanoclusters. *J. Am. Chem. Soc.* **2014**, *136*, 3624−3629.
(36) Calow, A. D. J.; Carbó, J. C.; Cid, J.; Fernández, E.; Whiting, A. Understanding α,β-unsaturated imine formation from amine additions to α,β-unsaturated aldehydes and ketones: an analytical and theoretical investigation. *J. Org. Chem.* **2014**, *79*, 5163−5172.
(37) Dabrowski, J. A.; Moebius, D. C.; Wommack, A. J.; Kornahrens, A. F.; Kingsbury, J. S. Catalytic and Regioselective Ring Expansion of Arylcyclobutanones with Trimethylsilyldiazomethane. Ligand-Dependent Entry to β-Ketosilane or Enolsilane Adducts. *Org. Lett.* **2010**, *12*, 3598−3601.
(38) Yu, K. P.; Sun, N.; Fang, S. Z.; Mo, W. M.; Hu, B. X.; Shen, Z. L.; Hu, X. Q. An Improved Process for the Preparation of Diphenylmethyl 7β-Phenylacetamido-3-hydroxymethyl-3-cephem-4-carboxylate. *Org. Process Res. Dev.* **2009**, *13*, 815−819.

https://dx.doi.org/10.1021/acs.oprd.0c00407
Org. Process Res. Dev. XXXX, XXX, XXX−XXX